

## ON THE STABILITY OF AIR CLATHRATE-HYDRATE CRYSTALS IN SUBGLACIAL LAKE VOSTOK, ANTARCTICA

**V.Ya. Lipenkov\*** and **V.A. Istomin<sup>†</sup>**

\* *Arctic and Antarctic Research Institute, 38 Bering St., St. Petersburg 199397, Russia*

<sup>†</sup> *Russian Research Institute of Natural Gases and Gas Technologies (VNIIGAZ),  
Moscovskaya Oblast 142717, Russia*

The conditions of air hydrate stability in Lake Vostok are quantified. The upper limit of concentration of O<sub>2</sub> dissolved in the subglacial water is predicted to be 50 times as high as the O<sub>2</sub> concentration in the air-supersaturated perennially ice-covered surface lakes in Antarctica.

### **1. Introduction**

Lake Vostok lying beneath ~4 km thick Antarctic ice sheet is the largest known subglacial lake on Earth, with dimensions of about 280 km × 50 km × 150 m. The ice-sheet base in contact with subglacial water body slopes from the south of the lake, where the ice thickness is 3775±15 m (in the vicinity of Vostok Station), to the north, where the ice-cover is approximately 4200 m thick [7] (see Fig. 1). Accordingly, the basal-ice melting prevails in the north of the lake, whereas the water freezing at the lake-ice interface occurs in the south [36, 38]. Convective circulation of lake water driven by geothermal and latent heat fluxes and the tilting of the ice ceiling supports the reallocation of ice from the thick-ice side to the thin-ice side of the lake, thereby helping to level the tilted ice sheet [46]. It has been shown that significant mass exchange between the overlying glacier ice and sub-ice water is one of Lake Vostok's major characteristics [20, 38, 46].

Consistent with the notion of water re-freezing at the southern end of the lake, a 200-250 m thick layer of accreted (lake) ice was discovered by deep coring performed at Vostok Station by the drilling group from the St. Petersburg Mining Institute [6, 22, 27]. In January 1998, drilling of the deepest 5G hole stopped at 3623 meters below the ice-

sheet surface (mbs), 85 m below the boundary between glacier and accreted ice, and ~150 m above the surface of Lake Vostok (Fig. 1). Microbiological studies of both glacier [12] and accreted [24, 33] sections of the Vostok ice core revealed a range of microbiota suggesting that viable microorganisms isolated from the rest of the biosphere for millions of years can potentially be found in Lake Vostok's water and bottom sediments. Environmental conditions, which may support a microbial population of Lake Vostok, become today the focus of scientific attention. Among other problems, the availability of oxygen for the bacterial metabolic processes that could operate in sub-ice water is currently under debate.

Glacier ice overlying the lake is characterized by abundance of air bubbles trapped during pore closure near the surface of the ice sheet. As the ice pressure increases with depth, the air occluded in ice gradually transforms to mixed air clathrate hydrate embedded in ice matrix as transparent sometimes beautifully faceted crystals or polycrystalline inclusions, with a typical size of 100-200  $\mu\text{m}$  [26] and cubic crystallographic structure II [17]. In the region of interest, the bubble-to-hydrate transition is complete at about 1300 mbs [26], below which depth most of the air in the ice sheet ( $\geq 99\%$ ) is located within hydrate crystals [18]. The total gas content of glacier ice at Vostok is about  $0.09\text{ cm}^3\text{ g}^{-1}$  (the gas volume is given at standard conditions:  $T = 273.15\text{ K}$  and  $P = 0.1013\text{ MPa}$ ) [5, 31], whereas that of accreted ice is reported to be nearly zero [22]. This suggests a net transfer of the atmospheric air (in the form of gas hydrate) through the ice-sheet thickness to the Lake Vostok water.

Because Lake Vostok is essentially closed system, it was at first thought that perpetual release of atmospheric gases from the melting glacier ice would eventually result in supersaturation of both oxygen and nitrogen [13]. According to Miller's diagram [32], however, the dissociation pressure of air hydrate at in situ temperature lies well below calculated hydrostatic pressure in Lake Vostok, which implies the hydrate could remain stable in the lake, thus reducing the amount of gases in aqueous solution. Assuming the presence of hydrates significantly restricts oxygen availability for biogeochemical reactions [40], sub-oxic conditions and prevalence of anaerobic microorganisms could be expected in the lake. In summary, "establishing the role of gas hydrate in Lake Vostok may be critical to understanding the subglacial ecosystem" [40].

In this study, we focus on conditions of air-hydrate stability in Lake Vostok. We also estimate the limit to which the potential persistence of air hydrate in the lake could reduce the amount of oxygen dissolved in sub-ice water. Finally, a plausible range of the O<sub>2</sub> concentration in Lake Vostok is discussed with respect to the O<sub>2</sub> content in other aquatic ecosystems.

## **2. Three-phase equilibria in the system atmospheric air – water**

It is assumed that Lake Vostok is composed of pure [14] or almost pure [23, 39] water. The gas content of the lake is substantially determined by two major atmospheric gases nitrogen and oxygen that have been released into water from the melting glacier ice (the ratio of N<sub>2</sub> to O<sub>2</sub> is taken to be 3.7). Based on available laboratory data and theoretical calculations, in this section we consider the three-phase equilibria: GLH, GHI, LHI, and GLI (where G - gas mixture of N<sub>2</sub> and O<sub>2</sub>, L - liquid water, H - hydrate structure II, and I - ice I<sub>h</sub>) in the system atmospheric air – water in the proximity of 0 °C, that is under thermodynamic conditions prevailing at the base of the Antarctic ice sheet.

### **Experimental and theoretical data on stability fields of N<sub>2</sub>, O<sub>2</sub> and air hydrates.**

The decomposition lines for O<sub>2</sub>, N<sub>2</sub> and air hydrates have been measured by a number of researchers [2, 21, 25, 32, 42, 43]. The data available for the temperature range of interest are gathered in Fig. 2 a-f; the corresponding references could be found in the figure caption. In general, the disagreement between different data sets for N<sub>2</sub> and O<sub>2</sub> pure hydrates does not exceed 4% in terms of pressure, well within expected errors of the experiments. The maximum uncertainties are observed in the decomposition lines for pure nitrogen hydrate in equilibrium with ice (Fig. 2d). The laboratory data given in the pioneer works by Van Cleef and Diepen [42, 43] (shown by dots) appear to underestimate (by 0.2 MPa on average) the dissociation pressure of N<sub>2</sub> hydrate as compared to both experimental curve from Miller [32] (dashed line) and more recent measurements by Kuhs and others [25] (solid line).

A first approximation of the dissociation pressure  $P_{d(\text{mix})}$  of a mixed gas hydrate may be obtained assuming that clathrate hydrate behaves as an ideally dilute solution and

that the ratio of occupancies for the small and large cages is constant and same for all guest molecules. Based on the statistical thermodynamic theory [44], the  $P_{d(mix)}$  for mixture of  $n$  gases can then be written (e.g., [9])

$$P_{d(mix)} = \left[ \sum \frac{y_i}{P_{di}} \right]^{-1}, \quad (1)$$

where  $P_{di}$  is the dissociation pressure of pure  $i$ -component of the gas mixture, and  $y_i$  is the mole fraction of this component in the gas phase. Applying Equation (1) to the atmospheric air ( $i = N_2, O_2$ ), the pressure  $P_{d(air)}$  at which the air hydrate begins to form can be approximated by

$$P_{d(air)} = \frac{P_{dN_2} P_{dO_2}}{y_{N_2} P_{dO_2} + y_{O_2} P_{dN_2}}. \quad (2)$$

Note that the latter equation [35] gives slightly different and more accurate values of  $P_{d(air)}$  than the equation previously suggested by Miller [32]. The validity of this simplified approach with respect to air hydrate is further supported by the fact that computations of  $P_{d(air)}$  from Equation (2) give nearly the same results as those obtained with more rigorous thermodynamic computation algorithm developed for prediction of the dissociation pressure of multi-component gas mixtures [9].

Equation (2) has been used to calculate the decomposition lines for mixed air hydrate in equilibrium with both ice and water (see Fig. 2c, f). Within the narrow temperature range considered here, the obtained three-phase curves can be represented by the following empirical relation:

$$\log_{10} P_d = A + B/T, \quad (3)$$

where  $P_d$  is given in MPa and  $T$  in K. Based on the data reported by Van Cleef and Diepen [42, 43] for pure  $N_2$  and  $O_2$  in equilibrium with liquid water, for the equilibrium air – water – air hydrate we estimate:  $A = 13.186$ ,  $B = -3279$ , including the metastable

extension of the GLH curve for supercooled water (shown by dotted line in Fig. 2c). With recent data from Kuhs and others [25] for pure N<sub>2</sub> and O<sub>2</sub> in equilibrium with ice, Equation (2) leads to the air – air hydrate – ice equilibrium curve as shown by dashed line 2 in Fig. 2f (corresponds to  $A = 3.875$  and  $B = -745.8$  in Equation (3)). The calculated curve overestimates the dissociation pressures by 4% with respect to the direct measurements [25] providing the only available up to now data on stability field of mixed air hydrate (see curve 1 in Fig. 2f corresponding to  $A = 3.63$ ,  $B = -683$ ).

It is worth noting that, for gases such as N<sub>2</sub> and O<sub>2</sub> with only slightly different dissociation pressures, Equation (1) approximates  $P_{d(mix)}$  with an accuracy of 5% or better at moderate pressures in the vicinity of the quadruple point. More rigorous consideration of the three-phase equilibria GLH and GHI for mixed gas hydrates taking into account real thermodynamic properties of the gas phase (e.g., Istomin [9]) shows that Equation (2) may indeed overestimate dissociation pressure of mixed air hydrate by a maximum of 2%. The remaining 2% in the discrepancy between calculated (curve 2) and measured (curve 1) decomposition lines in Fig. 2f can be attributed to the experimental uncertainties. Finally, the middle decomposition line (bold curve 3 in Fig. 2f) giving the average values of pressures as compared to curves 1 and 2 is assumed to equal the dissociation pressure of air hydrate in equilibrium with ice. The corresponding parameters in Equation (3) then are:  $A = 3.752$ ,  $B = -714.4$

### **The pressure melting temperature of Antarctic ice**

Ordinarily applying the equation of Clapeyron – Clausius to the case of pure water, one obtains a slope of  $dT / dP \approx -0.075 \text{ K MPa}^{-1}$  for the crystal-melt equilibrium in the single-component system. Consequently, the depression of the freezing (melting) temperature  $T_f$  of ice with pressure can be approximated by (e.g., [1]):

$$T_f(S, P) = T_f(S, 0) - 7.53 \cdot 10^{-2} P(\text{MPa}), \quad (4)$$

where  $S$  is the salinity. The relation (4) for pure water ( $S=0$ ,  $T_f(S, 0) \approx 273.15 \text{ K}$ ) is shown in Fig. 3 by dotted line 1. With sufficient accuracy, this relation also describes the properties of waters with low concentrations of gases, such as those at 1 atm.

In the case of Antarctic ice, however, a more accurate treatment of the pressure dependent freezing temperature involving consideration of gases dissolved in the melt water is needed. As a first approach, a linear extrapolation of the  $T_f - P$  relationship, obtained for water saturated with air at moderate pressures, to high pressures within hydrate stability field has been proposed [30] (see dashed line 2 in Fig. 3). The line has a slope of  $dT_f / dP \approx -0.098 \text{ K MPa}^{-1}$  which is often used to estimate the melting temperature at the bottom of ice sheets [30, 34]. However, air reaches a maximum of solubility at the three-phase equilibrium GLH (see below). Within field of air hydrate stability, the  $T_f - P$  curve should coincide with the equilibrium liquid (air-saturated) water – air hydrate – ice (LHI). Using the data on the LHI equilibrium for pure nitrogen and oxygen from Van Cleef and Diepen [42, 43] (shown by solid and open circles in Fig. 3) and assuming a linear form of the equilibrium curves, we estimate  $dT_f / dP = -0.079 \pm 0.001 \text{ K MPa}^{-1}$  for water + hydrate domain. Resultant  $T_f - P$  relation is shown in Fig. 3 by bold line 3.

For a given freezing temperature, the distance between two different water – ice (LI) equilibrium curves, corresponding one to gas-free water and another to the water with dissolved air, is determined by

$$P_{LI}(0) - P_{LI}(x_{air}) = -\frac{RT \ln(1 - x_{air})}{\Delta V_w} \approx \frac{RTx_{air}}{\Delta V_w}, \quad (5)$$

where  $x_{air}$  is the mole fraction of air in aqueous solution (the sum of the mole fractions of nitrogen and oxygen dissolved in water,  $x_{air} = x_{N_2} + x_{O_2}$ ),  $P_{LI}(0)$  and  $P_{LI}(x_{air})$  are the pressures taken at a fixed temperature on the corresponding LI equilibrium curves,  $R = 8.314 \text{ J mol}^{-1} \text{ K}^{-1}$  is the gas constant, and  $\Delta V_w$  is the difference between molar volume of water in ice and that in a liquid phase (under  $P, T$  conditions of interest,  $\Delta V_w \approx 1.64 \text{ cm}^3 \text{ mol}^{-1}$ ). Equation (5) can also be applied to theoretically predict the distance ( $P_{LI} - P_{LHI}$ ) between curve 1 (gas-free water – ice equilibrium) and LHI equilibrium line (shown in Fig. 3 as curve 4), in which case  $x_{air} = X_{air}$ , where  $X_{air}$  is the solubility of air in water in equilibrium with air hydrate. We address this question below.

### Equilibrium concentrations of N<sub>2</sub>, O<sub>2</sub> and air in water at high pressures

Out of hydrate stability field, in a solution in equilibrium with a free gas phase, the solubility of *i*-gas,  $X_i$ , and gas mixtures can be obtained from the equation of Krichevskii-Kazarnovskii [4]

$$X_i(P, T) = \frac{f_i}{H_i} \exp\left(-\frac{PV_i}{RT}\right), \quad (6)$$

where  $f_i$  is the fugacity,  $H_i$  is the temperature dependent Henry coefficient, and  $V_i$  is the partial molar volume of *i*-gas in a dilute solution;  $P$  denotes the total gas pressure in the system. Using Equation (6) with  $V_{N_2} = V_{O_2} = 32 \text{ cm}^3 \text{ mol}^{-1}$  and setting appropriate values for  $f_i$  and  $H_i$  as detailed in [10,19], we first calculate solubilities of N<sub>2</sub> and O<sub>2</sub> in supercooled water at -3°C (see curves 2 in Fig. 4), also extending our calculations over metastable conditions when a hydrate phase is still absent despite  $P > P_{d(air)}$  (curves 3 in Fig. 4). A temperature of -3 °C has been chosen here as an appropriate estimate of mean temperature in the lake.

Moving away from the three-phase boundary into two-phase water + hydrate domain reduces the aqueous solubility of gas, resulting in a greater proportion of clathrate for a given gas content of the system and an increase in occupancy of gas molecules in the clathrate cages [8]. A first approximation of solubility of N<sub>2</sub> and O<sub>2</sub> in a solution in equilibrium with air hydrate can be obtained using the following formula adopted from Istomin and Kwon [11]:

$$X_i(P, T) \approx X_i(P_{d(air)}) \exp\left[-\frac{\mathbf{a}(P - P_{d(air)})}{RT}\right], \quad (7)$$

where  $X_i(P_{d(air)})$  is the solubility of N<sub>2</sub> (or O<sub>2</sub>) at the three-phase boundary deduced at the previous step of our calculations. Note that for  $T = 270.15 \text{ K}$ , we should use  $P_{d(air)} = 11.17 \text{ MPa}$  which applies to metastable part of the GLH equilibrium curve shown

in Fig. 2c by dotted line. In Equation (7),  $\mathbf{a} = V_i - \frac{\Delta V_i}{\mathbf{n}_1 + \mathbf{n}_2} = 4.65 \dots 5.0 \text{ cm}^3 \text{ mol}^{-1}$ , where

$\Delta V_i \approx 4.8 \text{ cm}^3 \text{ mol}^{-1}$  is the difference between the partial molar volumes of  $\text{N}_2$  ( $\text{O}_2$ ) in the hydrate and liquid phases;  $n_1 = 2/17$  and  $n_2 = 1/17$  are the constants of hydrate structure II. As far as no gas phase is present in the system, the pressure  $P$  in Equation (7) has a meaning of hydrostatic pressure.

Based on Equation (7), we have calculated solubility of nitrogen and oxygen at a fixed temperature of 270,15 K and pressures exceeding the dissociation pressure of air hydrate. Between  $P_{d(\text{air})}$  and the pressure of ice freezing ( $P_f = 35.0 \text{ MPa}$  at  $-3^\circ\text{C}$ , see also Fig. 3), computed solubilities (curves 4 in Fig. 4) apply to metastable conditions of supercooled water in equilibrium with a hydrate phase. Although the latter state seems implausible, an extension of the solubility curves  $X_i(P)$  with the aid of Equation (7) to pressures exceeding  $P_f$  should lead us to a realistic estimate of the solubility of air in lake water, in equilibrium with air hydrate but in the absence of a free gas phase. Finally we obtain:  $X_{\text{N}_2} \approx 1.45 \cdot 10^{-3}$  (in mole fraction),  $X_{\text{O}_2} \approx 0.75 \cdot 10^{-3}$ , and  $X_{\text{air}} \approx 2.2 \cdot 10^{-3}$  at  $P = 35 \dots 40 \text{ MPa}$  and  $T = 270.15 \text{ K}$ , the conditions prevailing in Lake Vostok. These values determine an upper limit of air concentration in the lake water.

With the solubility deduced above, one can obtain from Equation (5):  $(P_{LI} - P_{LHI}) = 3 \text{ MPa}$  at  $-3^\circ\text{C}$ . Taking Equations (4) to calculate  $P_{LI}$ , we come to an estimate of  $P_{LHI} = 37 \text{ MPa}$  for the same temperature. This new point together with the quadruple point of the system air – water (13.3 MPa,  $-1.3^\circ\text{C}$ , see below) lead us to a new  $T_f - P$  linear relation (shown by thin line 4 in Fig. 3) with a slope of  $dT_f / dP = -0.073 \text{ K MPa}^{-1}$ , which is only slightly less than  $dT_f / dP = -0.079 \text{ K MPa}^{-1}$  based on the data set from Van Cleef and Diepen [42, 43]. The divergence of the two lines reaches about  $0.15^\circ\text{C}$  in terms of temperature and 2 MPa in terms of pressure at  $P, T$  conditions in Lake Vostok. Apart from uncertainties in the experimental data [42, 43] and our calculations, the expected nonlinearity of the LHI equilibrium curve should account for the small disagreement observed.

### **P-T diagram of air clathrate-hydrate near $0^\circ\text{C}$**

Resultant phase diagram for the system atmospheric air – pure water (Fig. 5) has been constructed as follows. The three-phase equilibria air – water – air hydrate (GLH) and air – air hydrate – ice (GHI) are given by Equation (3) with the coefficients

$A = 13.186$ ,  $B = -3279$  and  $A = 3.752$ ,  $B = -714.4$ , respectively. From the above consideration we expect that the uncertainties in both decomposition lines do not exceed 2% in terms of pressure. The quadruple point is determined by the intersection of the equations (3) for the GLH and GHI curves, which yields  $T = 271.8$  K ( $-1.3^\circ\text{C}$ ),  $P = 13.3$  MPa.

The equilibrium air – water – ice (GLI) is drawn in Fig. 5 as a straight line connecting the point  $T = 273.15$  K,  $P = 0$  MPa with the quadruple point of the phase diagram. The GLI line corresponds to  $dT_f / dP \approx -0.097$  K MPa<sup>-1</sup>, which slope applies to pressures below the field of air hydrate stability (the latter is indicated by shaded region in Fig. 5). The three-phase equilibrium gas saturated water – air hydrate – ice (LHI) is approximated in our diagram by a straight line starting from the quadruple point and having a slope of about  $-0.076$  K MPa<sup>-1</sup>, the average of the experimental and theoretical slopes discussed above. The uncertainty of thus obtained LHI curve due to its nonlinearity does not exceed  $\pm 0.07$  K for temperature. A value of  $dT_f / dP = -0.076$  K MPa<sup>-1</sup> can be suggested to calculate the pressure freezing (melting) temperature of Antarctic ice in the case when concentration of air in water reaches its maximum determined by solubility of N<sub>2</sub> and O<sub>2</sub> in the presence of air hydrate (see Fig. 4).

A combined heat- and ice-flow model, constrained by measurements of temperature in the 3623-m Vostok borehole have been used to extrapolate the temperature-depth profile down to the ice-water interface at the reference site F [34, 36], and to predict that at the reference site M (A. N. Salamatin, personal communication). Dotted curves M and F in the phase diagram show the corresponding pressure-temperature profiles in the ice sheet and underlying lake water at the two reference sites. At both sites, the vertical temperature gradients in the lake water are assumed to equal zero [46]. The pressure is calculated as a function of depth taking a mean density of ice of  $\sim 915$  kg m<sup>-3</sup> [29] and that of water of  $\sim 1016$  kg m<sup>-3</sup> [46]. Applying these calculations, we construct a triangle (see darkened area in the diagram) which is thought to represent the range of temperatures and pressures prevailing in the subglacial lake. Fig. 5 implies that, under in-situ conditions in Lake Vostok, the air-hydrate crystals released from the melting ice would persist in lake water provided there is enough air present in the system for a hydrate phase to coexist with nitrogen and oxygen dissolved in the water.

### 3. Conditions of air hydrate stability in sub-ice water

When observing an air-hydrate crystal that liberates from ice after the ice specimen has been subjected to an eutectic melting in ethylene glycol (Fig. 6), one can easily imagine what such a liberation might look like at high pressure, low temperature and permanent darkness of subglacial lake. The equilibrium density of air hydrate varies from 980 to 1025 kg m<sup>-3</sup> depending on the cage filling (occupancy) and the gas composition of hydrate [41]. Under conditions appropriate for the subglacial lake, the density of hydrate is expected to be less than or equal to the density of lake water (1016±1 kg m<sup>-3</sup> [46]). But even with a density of 1050 kg m<sup>-3</sup>, the hydrate crystals up to those 200 µm in diameter would be kept in suspension in the water column due to the convective turbulence with a velocity scales of ~0.3 mm s<sup>-1</sup> predicted for Lake Vostok by Wüest and Carmak [46].

In the previous section, we mainly considered cases when air is present in quantities sufficient for hydrate or gas phase to be in equilibrium with air-saturated water or ice. Being essentially closed system, Lake Vostok is supplied with air through the ice-sheet thickness. Total gas content of the lake involves gases dissolved in water and, possibly, gases imprisoned as guest molecules in host lattice of clathrate hydrates. In this section, we switch our attention to conditions which could support the two-phase equilibrium hydrate+gas-saturated water in subglacial Lake Vostok. We neglect contributions from biogeochemical inputs and losses of dissolved gases (as yet unavailable) and base our consideration of the total (bulk) gas content of the lake solely on the data from air content measurements in glacier and accreted ices.

In the upper 2546-m section of the Vostok core, the total air content of ice was measured using three different analytical techniques with calibration based on the data from vacuum-volumetric method (absolute accuracy better than ±1.5%) [5, 31]. The recent extension of the air content record down to the bottom of the Vostok core (3611 mbs) was done using the most efficient melting-refreezing gas-extraction procedure coupled with barometric method of gas measurements (accuracy ±0.6%) [28]. The complete analysis of the new data will be published elsewhere. Here we only present important information related to this study.

The measurements show that, in the region of Vostok Station, the air content of glacier ice between 170 and 3538 mbs remains within ±5% of its mean value of 0.0893

$\text{cm}^3 \text{g}^{-1}$ . Major shift in air content of the ice core is observed at 3538 mbs. Within few tens of centimeters, the air content falls by two orders of magnitude indicating a sharp transition from glacier ice to refrozen lake water. It is worth noting that substantially constant air content of the glacier ice suggests no drastic changes in the ice-sheet thickness in the Lake Vostok area over the last million years (the age of the ice core at 3538 mbs as estimated from the air-hydrate crystal growth rates [6]).

With respect to gas content, the Vostok accreted ice, however, is not as uniform as the Vostok glacier ice. First, the gas measurements support existence of two distinct layers in the accreted ice stratum. The upper 70-m layer (3538-3609 mbs) characterized by presence of untidily disseminated bedrock inclusions [22], is thought to have been accreted over turbulent lake water [46]. The mean gas content in this layer is  $\sim 0.001 \text{ cm}^3 \text{ g}^{-1}$ . Deeper 3609 mbs, the ice core is extremely clear and its gas content, similar to that of monocrystalline ice grown in the laboratory, is found to be below the detection limit ( $5 \cdot 10^{-5} \text{ cm}^3 \text{ g}^{-1}$ ) of the analytical equipment used.

Second, the detailed measurements performed in the upper layer of refrozen lake water show that the mean gas content of ice in small samples ( $2 \times 2 \times 2 \text{ cm}$ ) containing visible mineral inclusions is one order of magnitude higher than that in adjacent "clean" ice. This observation supports the idea about incorporation of lake water into accreted ice by capture and subsequent freezing of liquid-water inclusions ("water pockets") [39]. Interestingly, transparent three-dimensional hydrate crystals typical for glacier ice have never been detected in the upper section of the accreted ice, even though if they existed in large number in the lake water they could be incorporated in the lake ice in the same way as the mineral inclusions. Instead, new hydrate is expected to nucleate and grow from aqueous solution when it becomes saturated or supersaturated with respect to air during freezing of an isolated water pocket [15]. Presumably, this hydrate looks similar to sludge ice or snow and thus will hardly be visible in the accreted ice.

Extremely low and uniform air content of ice in the lower section of the accreted stratum (from 3609 to 3611 mbs and likely down to the ice-water interface at  $\sim 3775$  mbs) rules out a significant involvement of liquid-water pocket formation in the freezing process. This deepest  $\sim 170$ -m section of the Vostok ice has likely been accreted at the maximum water depth in the south of the lake where a thin layer of stably stratified water below the ice ceiling has been predicted [46]. Because of this boundary layer, the

geothermal convection can not reach here the ice ceiling, thus making the ice accretion a purely molecular process [46].

Gases enter Lake Vostok together with glacier ice melt in the northern part of the lake. The bulk concentration of air,  $C_{air}$ , in the newly melted water equals the air content of glacier ice ( $\sim 0.09 \text{ cm}^3 \text{ g}^{-1}$ ). Considering the atmospheric air as a pseudo-component of the system with a constant bulk composition (the  $\text{N}_2/\text{O}_2$  ratio is 3.7), hereafter we will express  $C_{air}$  as a sum of the mole fractions of  $\text{N}_2$  and  $\text{O}_2$  present in the system both in aqueous solution and in a hydrate phase. Correspondingly, for the bulk concentration of air in the newly melted water we have  $C_{air} \approx 0.09 \text{ cm}^3 \text{ g}^{-1} \approx 7 \cdot 10^{-5}$  mole fractions. Given that Lake Vostok originates from the melting of glacier ice [22], the melting alone would merely maintain (but not boost) concentration of gases in sub-ice water. Therefore, in the simplified scenario assumed, a value of  $C_{air} = 7 \cdot 10^{-5}$  should be viewed as a lower limit of the total gas content of lake water.

Gases are added to the lake water during ice accretion that prevails in the northern part of Lake Vostok. Only in the case of water pocket formation, gases cannot diffuse back in the lake during freezing and therefore both bulk concentration and composition of air in such frozen pockets must be the same as in the lake water. Considering the difference between the air concentrations in the upper ( $C_{air} = 8 \cdot 10^{-7}$ ) and in the lower (we take  $C_{air} = 0$ ) sections of the accreted ice as a result of solely water pocket formation and taking  $C_{air} = 7 \cdot 10^{-5}$  for the water, we come to an upper estimate of  $\sim 1\%$  for the volume fraction of the frozen water pockets in the upper section of accreted ice stratum. Much higher volume fraction (30-58%) inferred from isotopic data [39] could be understood if the air concentration in lake water was 27-50 times lower than that in the glacier ice. Whatever the volume fraction of the water pockets, the process of ice accretion tends to raise gas content of Lake Vostok above its original level of  $C_{air} = 7 \cdot 10^{-5}$ . For instance, the accretion of  $4 \text{ mm yr}^{-1}$  of lake water [36] over a half of the lake area ( $7000 \text{ km}^2$ ) would add  $\sim 10^{-10}$  mole fractions of air per year to the bulk air content of the lake (calculated for a lake volume of  $2100 \text{ km}^3$ ).

Because of the efficient vertical mixing in the lake [46] and likely low rates of melting [36], a possible difference between the air concentrations in the newly melted water and in the ambient lake water is to be eliminated almost simultaneously with melting. If the resultant bulk concentration of air in the water is less than the air solubility

( $C_{air} < X_{air}$ ), the hydrate crystals released from the melting ice would have to dissolve in the lake. In this case, both the mole fraction,  $x_{air}$ , and the composition of air in aqueous solution would be exactly the same as those in the bulk ( $x_{air} = C_{air}$ ; and the N<sub>2</sub>/O<sub>2</sub> ratio is 3.7). The hydrates, however, would persist in the lake when  $C_{air} = X_{air}$ . In the latter case,  $x_{air} = X_{air}$  and the gas compositions of hydrate and water-rich phases are different. Under metastable conditions when  $x_{air} > X_{air}$ , the hydrate crystals would tend to grow, thus forcing the system to return to its equilibrium at  $x_{air} = X_{air}$ . Note that gas cannot exist as a free phase within the field of air-hydrate stability provided that water is present in excess. The conditions of the two-phase equilibrium between air hydrate and air-saturated water can be seen from Fig 7 that is a relevant part of the isothermal  $P$ - $C$  diagram for the air-H<sub>2</sub>O system.

From the above consideration it follows that, in the absence of significant biological and chemical contributions to a bulk gas budget of Lake Vostok, the mole fraction of air dissolved in water ( $x_{air}$ ) lies between  $7 \cdot 10^{-5}$ , the air concentration ( $C_{air}$ ) in the melted glacier ice, and  $\sim 2.2 \cdot 10^{-3}$ , the air solubility ( $X_{air}$ ) in water in the presence of air hydrate (as computed for a temperature of  $-3^\circ\text{C}$  and pressures between 35 and 40 MPa in section 2). Under the long-term mass balance between the input of the melt water and the accreted ice export, the bulk concentration of air in the lake is  $C_{air} = 7 \cdot 10^{-5} t_E / t_R$ , where  $t_E$  is the total duration of Lake Vostok's steady state and  $t_R$  is the renewal (residence) time of the lake (by definition,  $t_R = M / m$ , where  $M$  is the mass of lake water and  $m$  is the mass of the ice accreted per unit of time). Therefore, formation of new air hydrate and/or growth of the air-hydrate crystals released from the ice sheet can be expected at some point of the Lake Vostok history.

Lake Vostok could have appeared before [3] or after [37] the Antarctic ice sheet reached its current dimensions (15-20 million years ago). It is likely that during its long history, the lake experienced epochs when either melting or freezing was dominant, respectively, slowing down or promoting the accumulation of atmospheric gases in sub-ice water. Assuming a steady state and taking different values for the rates of water/ice mass exchange, the residence time of the lake water was estimated to be between 5 and 50 kyr [20, 23, 46]. Based on these estimates one can obtain  $t_E = 160$ -1600 kyr, the time needed for  $C_{air}$  to reach a value of  $2.2 \cdot 10^{-3}$ , which is a condition of air hydrate stability in the lake. It seems therefore quite possible that at present time the lake water is already

saturated with atmospheric gases melted out from the ice sheet. This would imply that concentrations of both oxygen and nitrogen dissolved in the lake water have reached the maximum level determined by the solubility of these gases in water in equilibrium with air hydrate.

#### 4. Discussion and conclusive remarks

The  $P$ - $\tilde{N}$  diagram shown in Fig. 7 covers the ranges of gas contents and pressures which can be expected in subglacial Lake Vostok. The slightly inclined boundary between the water domain, within which  $x_{air} = C_{air} < X_{air}$ , and the water + hydrate domain ( $x_{air} = X_{air} \leq C_{air}$ ) corresponds to the solubility of air ( $X_{air} = X_{N_2} + X_{O_2}$ ) in equilibrium with a hydrate phase, according to Fig. 4. The inclined boundary that separates water-rich phase from the ice + hydrate domain is drawn as a function of  $x_{air}$ , according to Equation (5). The three-phase boundary between ice + hydrate and water + hydrate domains is flat because the mole fraction of air in aqueous solution in equilibrium with hydrate is constant at constant temperature and pressure. Finally, on the left-hand edge of the ice + hydrate domain, one can see a boundary, leftward of which an extremely low concentration of air ( $C_{air} < 6 \cdot 10^{-7}$ ) does not permit of a hydrate phase to be stable in ice, according to estimates of the solubility of air in ice in equilibrium with an air hydrate [18].

The diagram in Fig. 7, as well as all previous consideration, is based on the assumption that nitrogen and oxygen (with  $N_2/O_2$  ratio of 3.7) released from the melting glacier ice are the only gas constituents present in the Lake Vostok (pure) water. A significant geothermal activity in Lake Vostok's valley, which might be another source of gases in the lake water, is ruled out by recent helium isotope studies [20]. Although little is known about biological production (consumption) of  $O_2$  and possibly other gases in the lake, one can expect that gases such as  $CO_2$  and  $CH_4$  may also be present there in appreciable quantities. The stability conditions of  $CO_2$  and  $CH_4$  hydrates including natural hydrates in marine sediments and solubilities of these gases in water have been studied both experimentally and theoretically in great details (see e.g., [16] for  $CH_4$ ). Even small quantities of these strong hydrate-forming gases present together with  $N_2$  and  $O_2$  in the lake water could change significantly the GLH equilibrium curve with respect

to that indicated in Fig. 5. The calculations performed using the program for prediction of the dissociation pressure of multi-component gas mixtures [9] show that, with 0.01 mole fraction of CH<sub>4</sub> (CO<sub>2</sub>) in the bulk gas content of the lake system, the equilibrium pressures corresponding to the GLH curve would be ~4% (~10%) lower than those in Fig. 5. One should not expect, however, that small quantities of CH<sub>4</sub> and CO<sub>2</sub> potentially present in sub-ice water can significantly shift the bounds of the two-phase equilibrium hydrate + gas saturated water, as depicted in Fig. 7. Also, taking into account the low level of lake water salinity ( $S < 1\%$ ) inferred from accreted ice chemistry [39] would imply only minor corrections [1, 15] in the equilibrium lines drawn in Fig. 5 and Fig. 7.

A short summary of our preliminary estimates of gas composition of the Lake Vostok water is given in Table. It can be seen that concentration of dissolved oxygen ranges from  $x_{O_2} = 1.5 \cdot 10^{-5}$ , the lower bound corresponding to the total gas content of the newly melted water ( $\tilde{N}_{air} = 7 \cdot 10^{-5}$ ), to  $x_{O_2} = 0.75 \cdot 10^{-3}$ , the upper bound corresponding to  $\tilde{N}_{air} = 2.2 \cdot 10^{-3}$ . Normally, polar ice contains air in much larger quantities than can be dissolved in the same mass of water at 1 atm. Consistent with this, expected minimal concentration of O<sub>2</sub> in sub-ice water is 1.5-2 times higher than that in pure water under ambient conditions and nearly equals the average O<sub>2</sub> concentration in air-supersaturated waters of perennially ice-covered Antarctic surface lakes (30 mg O<sub>2</sub> liter<sup>-1</sup> =  $1.7 \cdot 10^{-5}$  mole fractions of O<sub>2</sub>, as reported for Lake Hoare in Victoria Land [45]). The hydrate crystals entering the lake due to glacier ice melting will dissolve in the water until the mole fractions of dissolved O<sub>2</sub> and N<sub>2</sub> reach their upper limits determined by solubility of these gases in the presence of air hydrate.

The maximal concentration of dissolved O<sub>2</sub> can be reached in Lake Vostok provided the water exchange between the base of the ice sheet and the lake waters has been operating with present-day efficiency at least for the past 0.2-1.6 million years, a quite possible scenario. Once this has happened, the mole fraction of O<sub>2</sub> (N<sub>2</sub>) in aqueous solution becomes time invariable and only slightly changes within the water depending on pressure and temperature distributions in the lake. Further accumulation of atmospheric gases will inevitably increase the fraction of a hydrate phase in the lake water due to formation of a new air hydrate or/and growth of the hydrate crystals released from the overlying ice sheet. The estimated maximal concentration of dissolved O<sub>2</sub> in Lake Vostok

is about 50 times as high as that in air-supersaturated ice-covered surface lakes in Antarctica.

Except for the small stratified water pull that likely exist below the southern (deepest) part of the lake, Lake Vostok is thought to be a well mixed water body because of the efficient water circulation driven by internal and geothermal heat fluxes [46]. In the present study, we certainly followed this “turbulent image” of Lake Vostok. However, it is also possible that near-bottom waters of the lake are more stagnant than it is assumed and therefore bear signature of the lake floor rather than its ceiling. If this is the case, our predictions are only valid for the upper waters that are entirely involved in the mass exchange occurring between the lake and the ice sheet.

A more rigorous and detailed consideration of the role of hydrates in the Lake Vostok hydrological system requires additional information on both gas composition and gas content of Lake Vostok's waters, the data to be still acquired in the course of ongoing accreted ice studies.

### Acknowledgments

We thank Prof. A.N. Salamatin for computing the temperature-depth profile in the ice sheet at the northern end of Lake Vostok and for valuable suggestions which helped to improve the paper. This work has gained much from useful discussions with colleagues at the International Conference on Conservation and Transformation of Matter and Energy in the Earth Cryosphere, Session: Gas Hydrates and Natural Gases in the Earth Cryosphere (June 1-5, 2001, Pushchino, Russia). The study was supported by grant N 99-05-65685 from the Russian Basic Research Foundation.

### References

1. Lipenkov A.N., Istomin A.A. *Antarctic Journal of the US*, 1998, 153 n.
2. Yá. Á., Á. Á. Ó. *Antarctic Journal of the US*, 1977, c. 1921.



14. Gorman M.R., Siegert M.J. Penetration of Antarctic subglacial water masses by VHF electromagnetic pulses: estimates of minimum water depth and conductivity. – *J. Geophys. Res.*, v. 104, N B12, 1999, p. 29311-29320.
15. Handa Y.P. Effect of hydrostatic pressure and salinity on the stability of gas hydrates. – *J. Phys. Chem.*, v. 94, 1990, p. 2653-2657.
16. Henry P., Thomas M., Clennell M.B. Formation of natural gas hydrates in marine sediments 2. Thermodynamic calculations of stability conditions in porous sediments. – *J. of Geophys. Res.*, v. 104, N B10, 1999, p. 23005-23022.
17. Hondoh T, Anzai H., Goto A., Mae S., Higashi A., Langway C.C. Jr. The crystallographic structure of the natural air-hydrate in Greenland Dye 3 deep ice core. – *J. Incl. Phenom. Mol. Recog. Chem.*, v. 8, N 1-2, 1990, p. 17-24.
18. Ikeda T., Salamatin A.N., Lipenkov V.Ya., Hondoh T. Diffusion of air molecules in polar ice sheets. – *Physics of Ice Core Records*, T. Hondoh (Ed.), Hokkaido University, 2000, p. 393-421.
19. Istomin V., Kwon V., Kulushev N., Kulkov A. Prevention of gas hydrate formation at field conditions in Russia. – *Natural Gas Hydrates. Proceedings of 2nd International Conference (June 2-6, 1996, Toulouse, France)*, 1996, p. 399-406.
20. Jean-Baptiste P., Petit J.R., Lipenkov V.Ya., Raynaud D., Barkov N.I. Constraints on hydrothermal processes and water exchange in Lake Vostok from helium isotopes. – *Nature*, v. 411, 2001, p. 460-462.
21. Jhavery J., Robinson D.B. Hydrates in the Methane-Nitrogen system. – *Can. J. Chem. Eng.*, v. 43, N 2, 1965 pp. 75-78.
22. Jouzel, J., J.R. Petit, R. Souchez., N.I. Barkov, V.Ya. Lipenkov, D. Raynaud, M. Stievenard, N.I. Vassiliev, V. Verbeke, F. Vimeux. More than 200 meters of lake ice above subglacial lake Vostok, Antarctica. – *Science*, v. 286, 1999, p. 2138-2141.
23. Kapitsa A.P., Ridley J.K., Robin G. de Q., Siegert M.J., Zotikov I.A. A large deep freshwater lake beneath the ice of central East Antarctica. – *Nature*, v. 381, 1996, p. 684-686.

24. Karl D.M., Bird D.F., Bjorkman K., Houlihan T., Shackelford R., Tupas L. Microorganisms in the accreted ice of Lake Vostok, Antarctica. – *Science*, v. 286, 1999, p. 2144-2147.
25. Kuhs W.F., Klapproth A., Chazallon B. Chemical physics of air clathrate hydrates. – *Physics of Ice Core Records*, T. Hondoh (Ed.), Hokkaido University, 2000, p. 373-392.
26. Lipenkov V.Ya. 2000. Air bubbles and air-hydrate crystals in the Vostok ice core. – *Physics of Ice Core Records*, T. Hondoh (Ed.), Hokkaido University, 2000, p. 327-358.
27. Lipenkov V.Ya., Barkov N.I. Internal structure of the Antarctic Ice Sheet as revealed by deep core drilling at Vostok Station. – *Lake Vostok Study: Scientific Objectives and Technological Requirements. Abstracts of the International Workshop (March 24-26, 1998, Arctic and Antarctic Research Institute, St. Petersburg, Russia)*, 1998, p. 31-35.
28. Lipenkov V.Ya., Candaudap F., Ravoit J., Dulac E., Raynaud D. A new device for air content measurements in polar ice. – *J. Glaciol.*, v.41, N 138, 1995, p.423-429.
29. Lipenkov V.Ya., Salamatin A.N., Duval P. Bubbly-ice densification in ice sheets: II. Application. – *J. Glaciol.*, v.43, N 145, 1997, p.397-407.
30. Lliboutry L. How to model the waxing and waning of ice-sheets. – *GeoResearch Forum*, v. 3-4 (Dynamics of the Ice Age Earth: A modern perspective), 1998, p. 249-270.
31. Martinerie, P.,V. Lipenkov, D. Raynaud, J. Chappellaz, N.I. Barkov, Lorius C.. Air content paleo record in the Vostok ice core (Antarctica): A mixed record of climatic and glaciological parameters. – *J. of Geophysical Research*, v. 99, N D5, 1994, p. 10565-10576.
32. Miller S.L. Clathrate hydrates of air in Antarctic ice. – *Science*, v. 165, N 3892, 1969, p. 489-490.
33. Priscu J.C., Adams E.E., Lyons W.B. and 9 others. Geomicrobiology of subglacial ice above Lake Vostok, Antarctica. – *Science*, v. 286, 1999, p. 2141-2144.

34. Salamatin A.N. Paleoclimatic reconstructions based on borehole temperature measurements in ice sheets. Possibilities and limitations. – *Physics of Ice Core Records*, T. Hondoh (Ed.), Hokkaido University, 2000, p. 243-282.
35. Salamatin A.N., Hondoh T., Uchida T., Lipenkov V.Ya. Post-nucleation conversion of an air bubble to clathrate air-hydrate crystals in ice. – *J. Crystal Growth*, v. 193, 1998, p. 197-218.
36. Salamatin A.N., Vostretsov R.N., Petit J.R., Lipenkov V.Ya., Barkov N.I. Geophysical and paleoclimatic implications of the stacked temperature profile from the deep bore hole at Vostok Station (Antarctica). – *Mater. Glyatsiol. Issled.*, N 85, 1998, p. 233-240.
37. Siegert M.J., Dowdeswell J.A., Gorman M.R., McIntyre N.F. An inventory of Antarctic subglacial lakes. – *Antarctic Science*, N 8, 1996, p. 281-286.
38. Siegert M.J., Kwok R., Mayer C., Hubbard B. Water exchange between the subglacial Lake Vostok and the overlying ice sheet. – *Nature*, v. 403, 2000, p. 643-646.
39. Souchez R., Petit J.R., Tison J.-L., Jouzel J. and Verbeke V. Ice formation in subglacial Lake Vostok, Central Antarctica. – *Earth and Planetary Science Letters*, v. 181, 2000, p. 529-538.
40. Subglacial Lake Exploration. SCAR Workshop Report and Recommendations. Cambridge, 1999, 26 p.
41. Uchida T., Hondoh T. Laboratory studies on air-hydrate crystals. – *Physics of Ice Core Records*, T. Hondoh (Ed.), Hokkaido University, 2000, p. 423-457.
42. Van Cleef A., Diepen G.A.M. Gas hydrates of nitrogen and oxygen. – *Recueil Trav. Chim.*, v. 79, 1960, p. 582-586.
43. Van Cleef A., Diepen G.A.M. Gas hydrates of nitrogen and oxygen. II. – *Recueil Trav. Chim.*, v. 84, 1965, p. 1085-1093.
44. Van der Waals J.H. and Platteeuw J.C. Clathrate solutions. – *Adv. Chem. Phys.*, v. 2, N 1, 1959, p. 1-57.
45. Wharton R.A. Jr., McKay C.P., Simmons G.M. Jr., Parker B.C. Oxygen budget of a perennially ice-covered Antarctic lake. – *Limnology and Oceanography*, v. 31, 1986, p. 437-443.
46. Wuest A., Carmack E. A priori estimates of mixing and circulation in the hard-to-reach water body of Lake Vostok. – *Ocean Modelling*, N 2, 2000, p. 29-43.

Table

The properties of sub-ice water estimated for plausible range of the gas content of Lake Vostok

Quantity	Gas content of lake water	
	Min. ( $C_{air} = 7 \cdot 10^{-5}$ )	Max*. ( $C_{air} = 2.2 \cdot 10^{-3}$ )
Mole fraction of air in aqueous solution, $x_{air}$	$7 \cdot 10^{-5}$	$2.2 \cdot 10^{-3}$
Mole fraction of N <sub>2</sub> in aqueous solution, $x_{N_2}$	$5.5 \cdot 10^{-5}$	$1.45 \cdot 10^{-3}$
Mole fraction of O <sub>2</sub> in aqueous solution, $x_{O_2}$	$1.5 \cdot 10^{-5}$	$0.75 \cdot 10^{-3}$
Freezing temperature, $T_f$ (°C), at $P = 37.8$ MPa (melting site M)	-2.86	-3.15
Freezing temperature, $T_f$ (°C), at $P = 33.9$ MPa (freezing site F, Vostok Station)	-2.62	-2.85

\* When  $C_{air} = 2.2 \cdot 10^{-3}$ , air hydrate is in equilibrium with nitrogen and oxygen dissolved in lake water.

**Figure captions**

Fig. 1. Schematic cross section of the Antarctic ice sheet along the whole length of Lake Vostok. **M** and **F** are the reference sites at the northern end (melting zone) and at the southern end (freezing zone) of Lake Vostok, respectively. In very general terms, the sketch reproduces the glaciological setting of the subglacial lake as established by a number of researchers [7, 22, 23, 27, 38].

Fig. 2. Experimental and calculation data on the decomposition lines for  $N_2$ ,  $O_2$ , and air clathrate hydrates. The data and the quadruple points ( $Q_{N_2}$ ,  $Q_{O_2}$ ) from van Cleef and Diepen [42, 43] are shown by dots and crosses, respectively. (a) Gas-liquid water-hydrate (GLH) equilibrium in the system  $N_2 - H_2O$ ; the fits of the data from [2] (dashed curve) and from [21] (solid curve) are shown for comparison. (b) GLH equilibrium in the system  $O_2 - H_2O$ . (c) GLH equilibrium in the system air -  $H_2O$ : the decomposition curve is calculated from Equation (2) using the data from [42, 43]. (d) Gas-hydrate-ice (GHI) equilibrium in the system  $N_2 - H_2O$ ; solid and dashed curves are the fits of laboratory data obtained by Kuhs and others [25] and Miller [32], respectively. (e) GHI equilibrium in the system  $O_2 - H_2O$ ; the curves as in (d). (f) GHI equilibrium in the system air -  $H_2O$ : thin curve 1 shows experimental decomposition line from [25]; dashed curve 2 is calculated from Equation (2) on the basis of the data for pure  $N_2$  and  $O_2$  hydrates [25] presented in (d) and (e); curve 3 gives the middle values of the dissociation pressure as compared to curves 1 and 2.

Fig. 3. Freezing temperature of water as a function of pressure plotted for pure gas-free water and air-saturated water. 1 – gas-free water; 2 – linear extrapolation of the  $T_f - P$  relationship for air-saturated water to high pressures in the field of air hydrate stability; 3  $\blacklambda$  air-saturated water in equilibrium with hydrate (linear fit of laboratory data [42, 43]); 4  $\blacklambda$  same as 3, but the  $T_f - P$  line is calculated from Equations (4) and (5) as described in the main text; 5, 6 – data on the gas(hydrate)-ice-water equilibria in the systems  $N_2 - H_2O$  and  $O_2 - H_2O$ , respectively [42, 43]; 7

– the quadruple points for  $N_2$  ( $Q_{N_2}$ ) and  $O_2$  ( $Q_{O_2}$ ) hydrates [43]. The average conditions at the ice – lake water interface (35 MPa,  $-3$  °C) are indicated by thin dotted lines.

Fig. 4. Solubility of major air constituents in pure water at  $-3$  °C computed as a function of hydrostatic pressure (see text). 1 – solubility of nitrogen ( $X_{N_2}$ ) and oxygen ( $X_{O_2}$ ) in a solution in equilibrium with air hydrate. The values of  $X_{N_2}$  and  $X_{O_2}$  at pressures prevailing in Lake Vostok (indicated by shaded region) determine the upper limits of concentrations of respective gases in the lake water. Curves 2-4 illustrate the sequential steps of computation and predict solubility of  $N_2$  and  $O_2$  under the following metastable conditions: 2 – supercooled water; 3 – supercooled water at pressures exceeding the dissociation pressure ( $P_{d(air)} = 11.17$  MPa at  $-3$ °C) but in the absence of a hydrate phase; 4 – implausible case of supercooled water in equilibrium with a hydrate phase.

Fig. 5. The phase diagram of air clathrate hydrate near  $0$  °C. Dotted curves show the relations between temperature and pressure (depth) in the Antarctic ice sheet and sub-ice water at the reference sites **M** and **F** located in the zones of subglacial melting and freezing, respectively. Shaded region shows field of air hydrate stability. Small darkened triangle within this field covers the range of in-situ conditions in Lake Vostok.

Fig. 6. Air-hydrate crystal liberating from glacier ice into Lake Vostok, according to laboratory imitation experiment. (The photograph catches the moment when hydrate separates from ice specimen subjected to an eutectic melting in ethylene glycol.)

Fig. 7.  $P$ - $C$  section through the full  $P$ - $T$ - $C$  diagram of the air – water system for  $T = 270.15$  K and  $P = 30...45$  MPa. Shaded region shows the domain in which total gas content ( $C_{air}$ ) of the system is sufficient for air hydrate to be in equilibrium with gas-saturated water. Vertical dashed line shows the air content of Antarctic (glacier) ice ( $C_{air} = 7 \cdot 10^{-5}$ ).

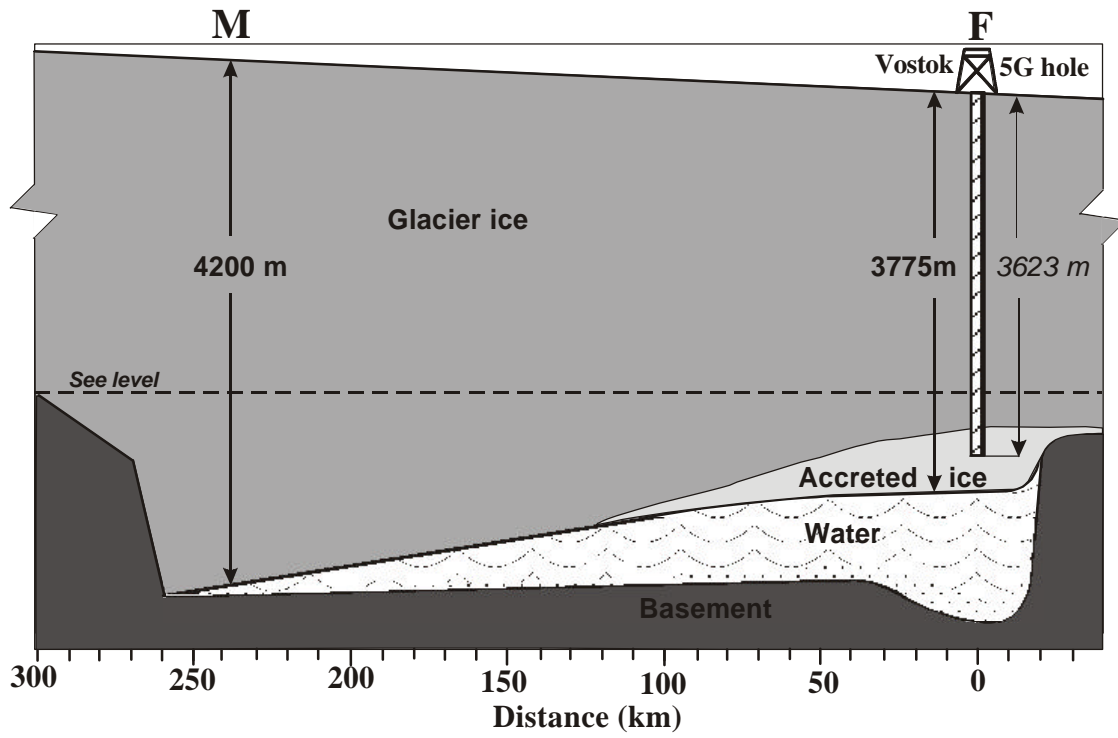


Fig. 1

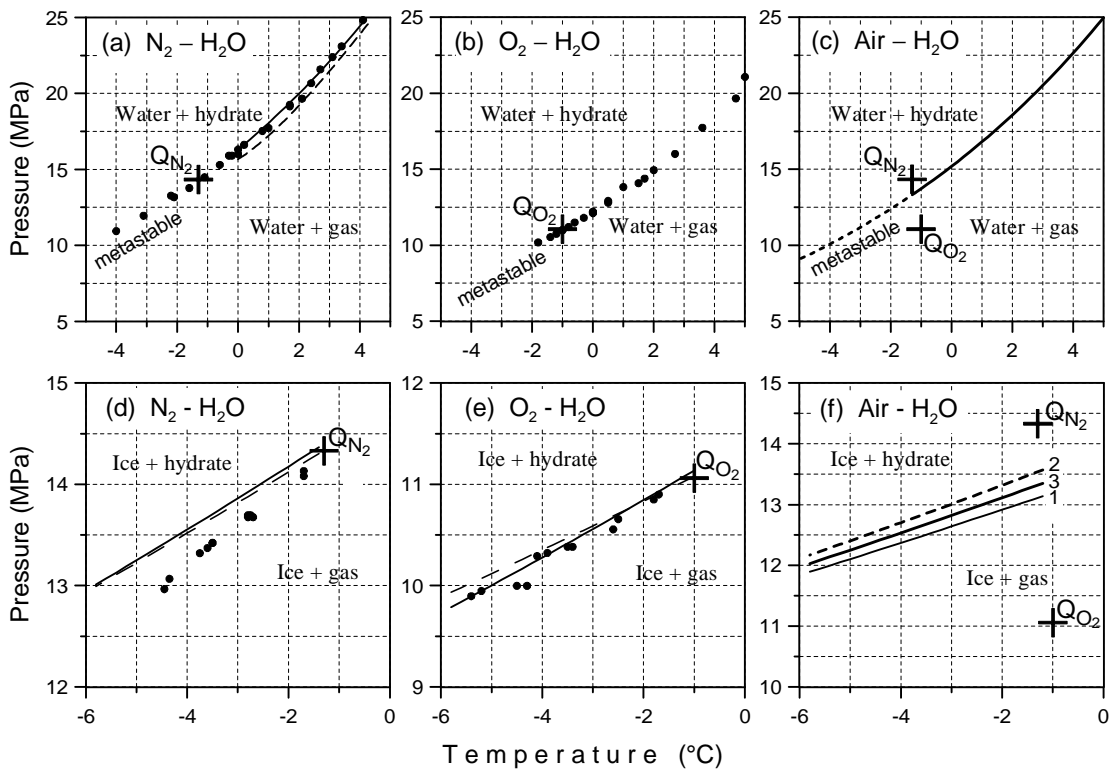


Fig.2

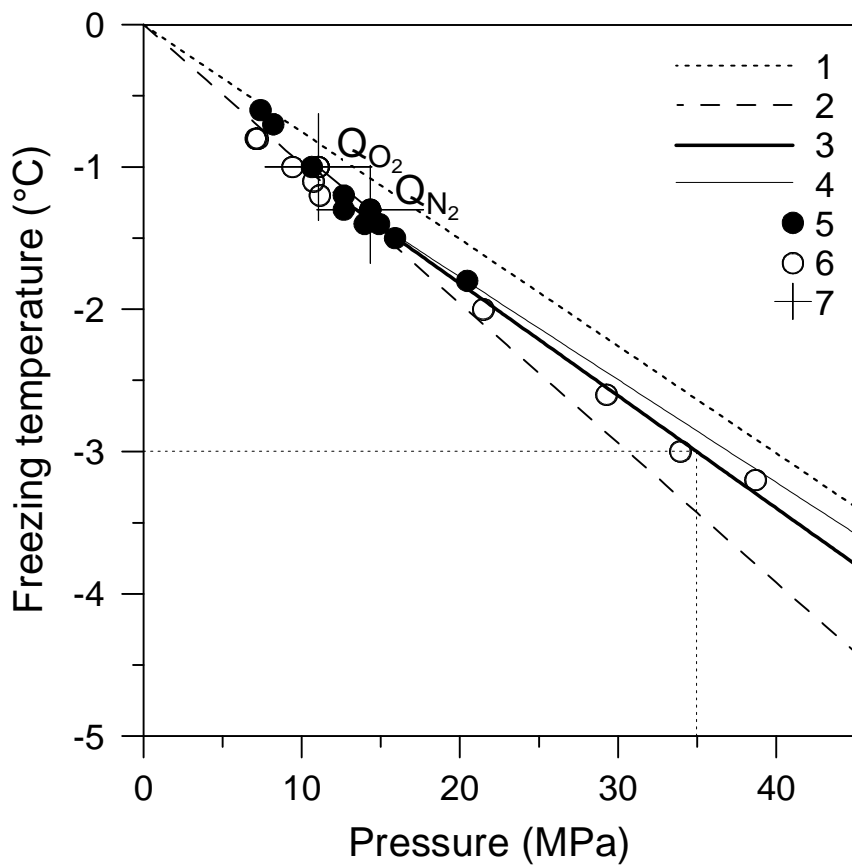


Fig.3

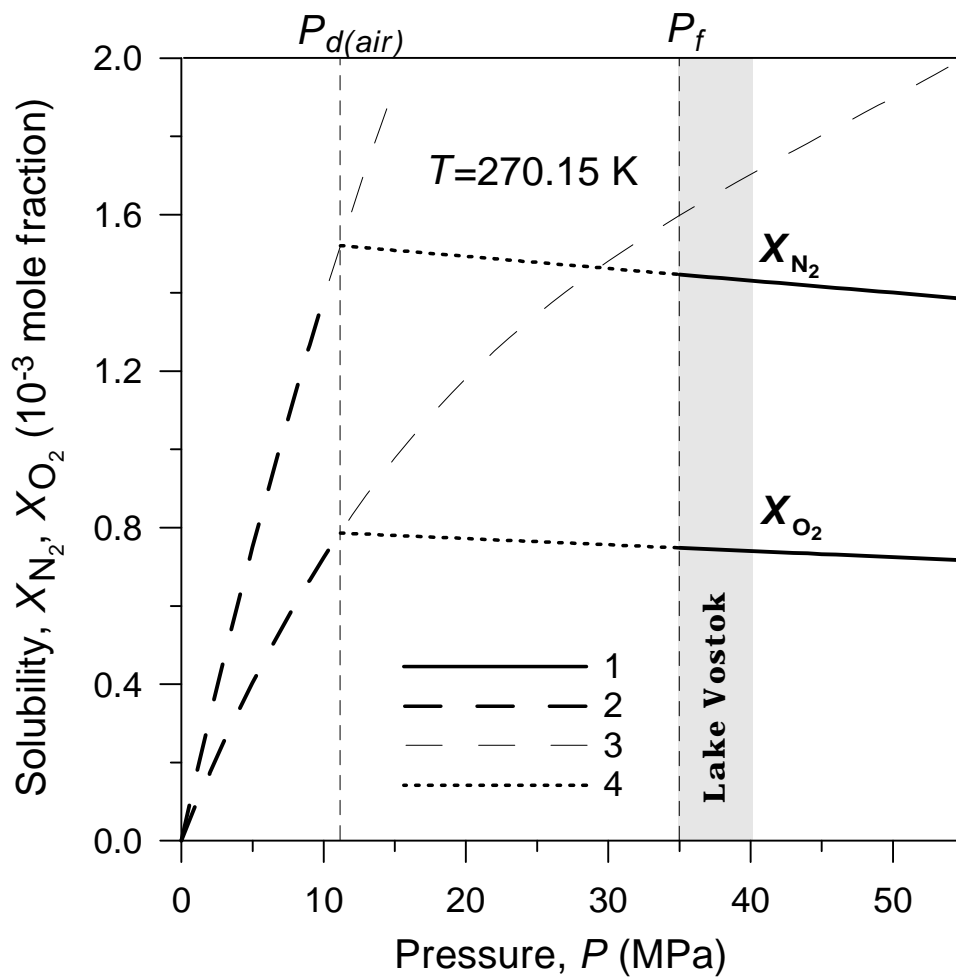


Fig.4

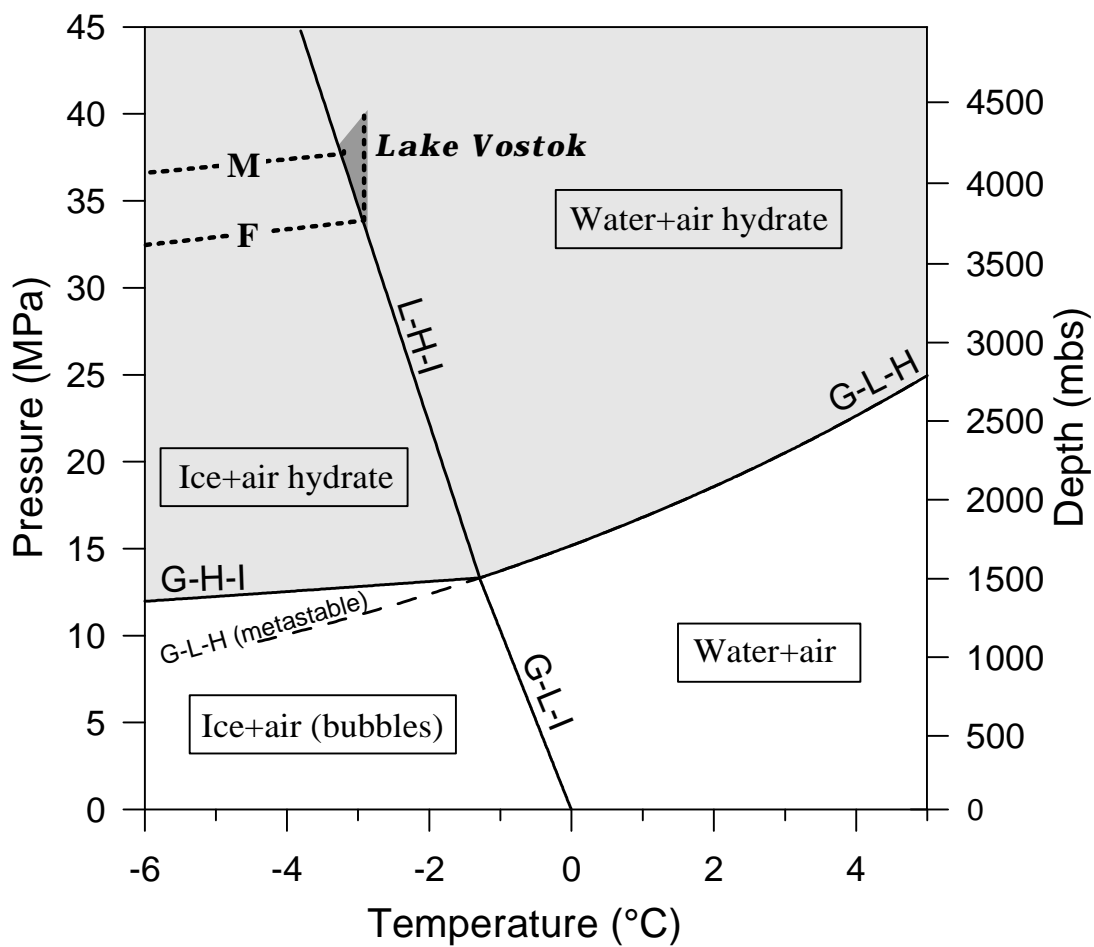


Fig. 5

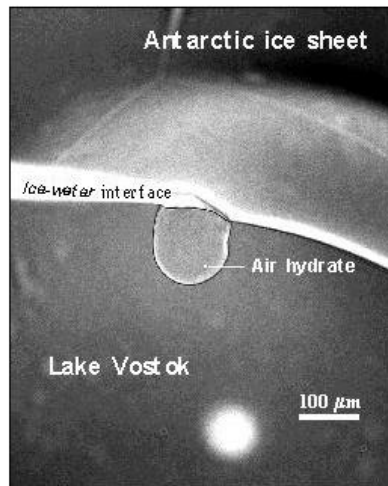


Fig. 6

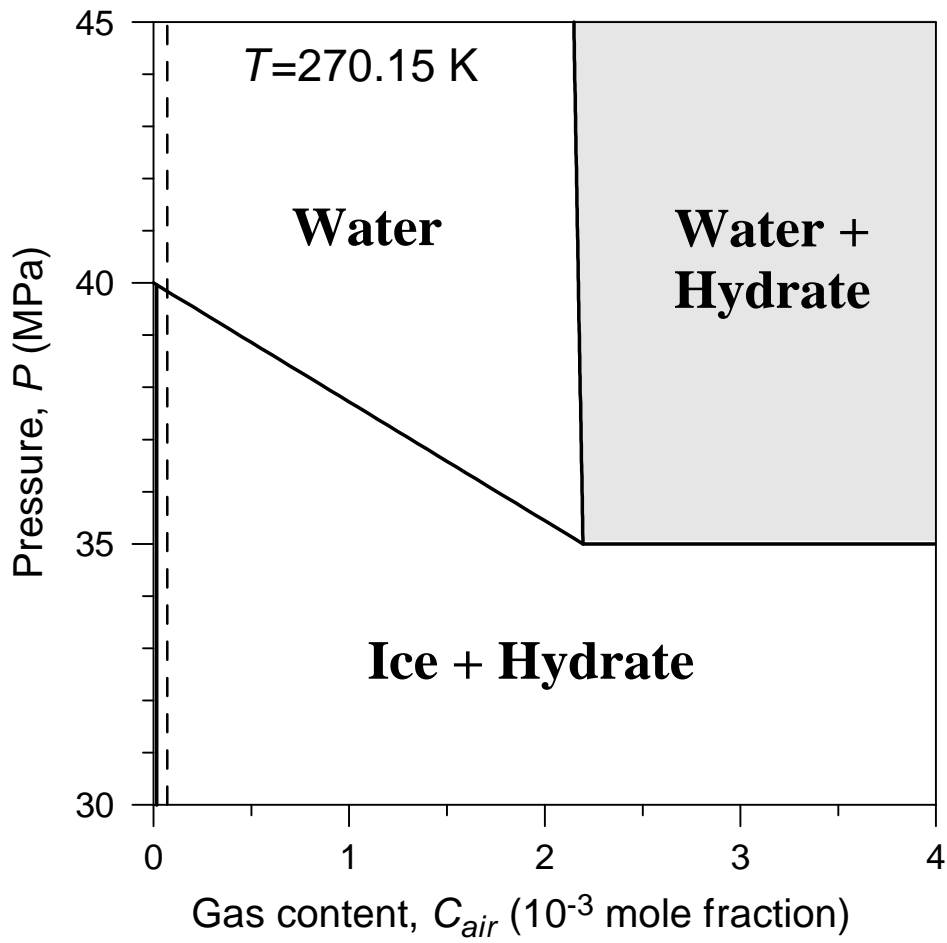


Fig.7